

Current Topics in Microbiology and Immunology

Volume 334

Series Editors

R. John Collier

Department of Microbiology and Molecular Genetics, Harvard Medical School,
200 Longwood Avenue, Boston, MA 02115, USA

Richard W. Compans

Emory University School of Medicine, Department of Microbiology
and Immunology, 3001 Rollins Research Center, Atlanta, GA 30322, USA

Max D. Cooper

Department of Pathology and Laboratory Medicine, Georgia Research Alliance,
Emory University, 1462 Clifton Road, Atlanta, GA 30322, USA

Yuri Y. Gleba

ICON Genetics AG, Biozentrum Halle, Weinbergweg 22, Halle 6120, Germany

Tasuku Honjo

Department of Medical Chemistry, Kyoto University, Faculty of Medicine, Yoshida,
Sakyo-ku, Kyoto 606-8501, Japan

Hilary Koprowski

Thomas Jefferson University, Department of Cancer Biology, Biotechnology Foundation
Laboratories, 1020 Locust Street, Suite M85 JAH, Philadelphia,
PA 19107-6799, USA

Bernard Malissen

Centre d'Immunologie de Marseille-Luminy, Parc Scientifique de Luminy, Case 906,
Marseille Cedex 9 13288, France

Fritz Melchers

Biozentrum, Department of Cell Biology, University of Basel, Klingelbergstr.
50-70, 4056 Basel Switzerland

Michael B.A. Oldstone

Department of Neuropharmacology, Division of Virology, The Scripps
Research Institute, 10550 N. Torrey Pines, La Jolla, CA 92037, USA

Sjur Olsnes

Department of Biochemistry, Institute for Cancer Research,
The Norwegian Radium Hospital, Montebello 0310 Oslo, Norway

Herbert W. "Skip" Virgin

Washington University School of Medicine, Pathology and Immunology, University Box
8118, 660 South Euclid Avenue, Saint Louis, Missouri 63110, USA

Peter K. Vogt

The Scripps Research Institute, Dept. of Molecular & Exp. Medicine, Division of
Oncovirology, 10550 N. Torrey Pines. BCC-239, La Jolla, CA 92037, USA

Current Topics in Microbiology and Immunology

Previously published volumes

Further volumes can be found at springer.com

- Vol. 309: **Polly Roy (Ed.):**
Reoviruses: Entry, Assembly and Morphogenesis. 2006. 43 figs. XX, 261 pp. ISBN 3-540-30772-9
- Vol. 310: **Doerfler, Walter; Böhm, Petra (Eds.):**
DNA Methylation: Development, Genetic Disease and Cancer. 2006. 25 figs. X, 284 pp. ISBN 3-540-31180-7
- Vol. 311: **Pulendran, Bali; Ahmed, Rafi (Eds.):**
From Innate Immunity to Immunological Memory. 2006. 13 figs. X, 177 pp. ISBN 3-540-32635-9
- Vol. 312: **Boshoff, Chris; Weiss, Robin A. (Eds.):**
Kaposi Sarcoma Herpesvirus: New Perspectives. 2006. 29 figs. XVI, 330 pp. ISBN 3-540-34343-1
- Vol. 313: **Pandolfi, Pier P.; Vogt, Peter K.(Eds.):**
Acute Promyelocytic Leukemia. 2007. 16 figs. VIII, 273 pp. ISBN 3-540-34592-2
- Vol. 314: **Moody, Branch D. (Ed.):**
T Cell Activation by CD1 and Lipid Antigens, 2007, 25 figs. VIII, 348 pp. ISBN 978-3-540-69510-3
- Vol. 315: **Childs, James, E.; Mackenzie, John S.; Richt, Jürgen A. (Eds.):**
Wildlife and Emerging Zoonotic Diseases: The Biology, Circumstances and Consequences of Cross-Species Transmission. 2007. 49 figs. VII, 524 pp. ISBN 978-3-540-70961-9
- Vol. 316: **Pitha, Paula M. (Ed.):**
Interferon: The 50th Anniversary. 2007. VII, 391 pp. ISBN 978-3-540-71328-9
- Vol. 317: **Dessain, Scott K. (Ed.):**
Human Antibody Therapeutics for Viral Disease. 2007. XI, 202 pp. ISBN 978-3-540-72144-4
- Vol. 318: **Rodriguez, Moses (Ed.):**
Advances in Multiple Sclerosis and Experimental Demyelinating Diseases. 2008. XIV, 376 pp. ISBN 978-3-540-73679-9
- Vol. 319: **Manser, Tim (Ed.):**
Specialization and Complementation of Humoral Immune Responses to Infection. 2008. XII, 174 pp. ISBN 978-3-540-73899-2
- Vol. 320: **Paddison, Patrick J.; Vogt, Peter K.(Eds.):** RNA Interference. 2008. VIII, 273 pp. ISBN 978-3-540-75156-4
- Vol. 321: **Beutler, Bruce (Ed.):**
Immunology, Phenotype First: How Mutations Have Established New Principles and Pathways in Immunology. 2008. XIV, 221 pp. ISBN 978-3-540-75202-8
- Vol. 322: **Romeo, Tony (Ed.):**
Bacterial Biofilms. 2008. XII, 299. ISBN 978-3-540-75417-6
- Vol. 323: **Tracy, Steven; Oberste, M. Steven; Drescher, Kristen M. (Eds.):**
Group B Cocksackieviruses. 2008. ISBN 978-3-540-75545-6
- Vol. 324: **Nomura, Tatsuji; Watanabe, Takeshi; Habu, Sonoko (Eds.):**
Humanized Mice. 2008. ISBN 978-3-540-75646-0
- Vol. 325: **Shenk, Thomas E.; Stinski, Mark F. (Eds.):**
Human Cytomegalovirus. 2008. ISBN 978-3-540-77348-1
- Vol. 326: **Reddy, Anireddy S.N; Golovkin, Maxim (Eds.):**
Nuclear pre-mRNA processing in plants. 2008. ISBN 978-3-540-76775-6
- Vol. 327: **Manchester, Marianne; Steinmetz, Nicole F. (Eds.):**
Viruses and Nanotechnology. 2008. ISBN 978-3-540-69376-5
- Vol. 328: **van Etten, (Ed.):**
Lesser Known Large dsDNA Viruses. 2008. ISBN 978-3-540-68617-0
- Vol. 329: **Diane E. Griffin; Michael B.A. Oldstone (Eds.):** Measles 2009. ISBN 978-3-540-70522-2
- Vol. 330: **Diane E. Griffin; Michael B.A. Oldstone (Eds.):** Measles 2009. ISBN 978-3-540-70616-8
- Vol. 331 **Villiers, E. M. de (Eds):**
TT Viruses. 2009. ISBN 978-3-540-70917-8
- Vol. 332 **Karasev A.(Ed.):**
Plant produced Microbial Vaccines. 2009. ISBN 978-3-540- 70857-5
- Vol. 333 **Richard W. Compans; Walter A. Orenstein (Eds):** Vaccines for Pandemic Influenza. 2009. ISBN 978-3-540-92164-6

Dorian McGavern • Michael Dustin
Editors

Visualizing Immunity

 Springer

Editors

Dr. Dorian McGavern
National Institutes of Neurological
Disorders and Stroke
National Institutes of Health (NIH)
10 Center Drive
Bldg 10, Rm 7C213
Bethesda, MD 20892
USA
mcgavernd@mail.nih.gov

Dr. Michael Dustin
New York University
School of Medicine
Skirball Institute of Biomolecular Medicine
540 First Ave.
New York NY 10016
USA
dustin@saturn.med.nyu.edu

ISBN 978-3-540-93862-0 e-ISBN 978-3-540-93864-4
DOI 10.1007/978-3-540-93864-4
Springer Dordrecht Heidelberg London New York

Current Topics in Microbiology and Immunology ISSN 0070-217x

Library of Congress Catalog Number: 2008944027

© Springer-Verlag Berlin Heidelberg 2009

This work is subject to copyright. All rights reserved, whether the whole or part of the material is concerned, specifically the rights of translation, reprinting, reuse of illustrations, recitation, broadcasting, reproduction on microfilm or in any other way, and storage in data banks. Duplication of this publication or parts thereof is permitted only under the provisions of the German Copyright Law of September, 9, 1965, in its current version, and permission for use must always be obtained from Springer-Verlag. Violations are liable for prosecution under the German Copyright Law.

The use of general descriptive names, registered names, trademarks, etc. in this publication does not imply, even in the absence of a specific statement, that such names are exempt from the relevant protective laws and regulations and therefore free for general use.

Product liability: The publisher cannot guarantee the accuracy of any information about dosage and application contained in this book. In every individual case the user must check such information by consulting the relevant literature.

Cover legend: Localization of cytotoxic lymphocytes (CTL) during fatal LCMV-induced meningitis.

This low magnification panel shows LCMV-specific CTL in green, meningeal blood vessels in red, and skull in blue. The 3D image was captured from a symptomatic mouse at day 6 post-infection using a two photon microscope. Virus-specific CTL tend to aggregate along meningeal blood vessels, because the stromal network that surrounds these vessels is infected by LCMV. This image was captured by Dr. Jiyun Kim at New York University.

Cover design: WMX Design GmbH, Heidelberg, Germany

Printed on acid-free paper

Springer is part of Springer Science+Business Media (www.springer.com)

Preface

Researchers have used a variety of techniques over the past century to gain fundamental insights in the field of immunology and, as technology has advanced, so too has the ability of researchers to delve deeper into the biological mechanics of immunity. The immune system is exceedingly complex and must patrol the entire body to protect us from foreign invaders. This requires the immune system to be highly mobile and adaptable - able to respond to diverse microbial challenges while maintaining the ability to distinguish self from a foreign invader. This latter feature is of great importance because the immune system is equipped with toxic mediators, and a failure in self/non-self discrimination can result in serious diseases. Fortunately, in most cases, the immune system operates within the framework of its elegant design and protects us from diverse microbial challenges without initiating disease.

Because the immune system is not confined to a single tissue, a comprehensive understanding of immunity requires that research be conducted at the molecular, cellular, and systems level. Immune cells often find customized solutions to handling microbial insults that depend on the tissue(s) in which the pathogen is found. Removal of immune cells from their natural environment is one common means by which immunity is studied; however, this approach comes with the caveat that immune cells interact uniquely with the microenvironments and tissue architecture they encounter. Because no two tissues are alike, immune cells will often adapt and respond based on the unique microenvironment in which they reside. Given this fact, it is of great importance to consider cellular context when deciphering the mysteries of the immune system. Lessons learned in one tissue may not necessarily apply to the entire body.

Understanding the contextual side of immunity necessitates study of immune cells *in vivo*. However, those that pursue *in vivo* research immediately encounter the obstacle of how best to study immune cells in their natural environments. This obstacle is not a trivial one, as it is far easier to remove cells from their natural environments and study them *ex vivo* or *in vitro*. Fortunately, scientists in other disciplines have come to the rescue with exciting advances in imaging techniques. These advances have enabled immunologists to quite literally “see” how immune cells respond to diverse challenges. Using static imaging approaches, researchers have captured snapshots in time, which are then pieced together with

corroborating datasets to assemble a sequence of events. More recently, researchers have instituted an exciting upgrade, transitioning from static to dynamic imaging techniques such as two-photon laser scanning microscopy. These dynamic approaches are advantageous because researchers can use them to study immune cells in their natural environments in real time. Thus, it is no longer necessary to extrapolate from *in vitro* observations how immune cells operate *in vivo*. Immune cells operating in states of health and disease can now be filmed and studied afterwards in great detail.

The field of visualizing immunity has moved rapidly over recent years and has carved out an important niche within the broader discipline of immunology. This issue was assembled to pay tribute to those who have gleaned fundamental insights in immunology using imaging approaches. The reviews within span a breadth of knowledge that covers certain technical, molecular, cellular, and systems aspects of visualizing immunity. The issue begins with what should be considered when assembling a custom imaging platform and then progresses to the mechanics of T cell interactions and activation. From there, the issue moves on to lymphocyte motility/migration, B lymphocyte activation, and finally to visualizations of some challenges that immune cells face (e.g., pathogens and tumors). We felt that these topics have a natural flow in the order presented and allow the reader to “see” the development of immune responses at all levels. The visualizations within are aesthetically pleasing, and it is gratifying to know that many novel insights have been extracted from such stunning imagery. Now that the field has been set ablaze with enthusiasm, it is certain that exciting new immunological discoveries lie just around the corner. This issue is merely a snapshot in time for a field that should grow exponentially in the years to come.

Dorian B. McGavern

Contents

Two-Photon Imaging of the Immune System: A Custom Technology Platform for High-Speed, Multicolor Tissue Imaging of Immune Responses	1
Andrew Bullen, Rachel S. Friedman, and Matthew F. Krummel	
Visualizing Intermolecular Interactions in T Cells	31
Nicholas R.J. Gascoigne, Jeanette Ampudia, Jean-Pierre Clamme, Guo Fu, Carina Lotz, Michel Mallaun, Nathalie Niederberger, Ed Palmer, Vasily Rybakin, Pia P. Yachi, and Tomasz Zal	
Multiscale Analysis of T Cell Activation: Correlating <i>In Vitro</i> and <i>In Vivo</i> analysis of the Immunological Synapse	47
Michael L. Dustin	
T Cell Migration Dynamics Within Lymph Nodes During Steady State: An Overview of Extracellular and Intracellular Factors Influencing the Basal Intranodal T Cell Motility	71
Tim Worbs and Reinhold Förster	
Chemoattractant Receptor Signaling and Its Role in Lymphocyte Motility and Trafficking	107
John H. Kehrl, Il-Young Hwang, and Chung Park	
New Insights Into Leukocyte Recruitment by Intravital Microscopy	129
Alexander Zarbock and Klaus Ley	

Visualizing the Molecular and Cellular Events Underlying the Initiation of B-Cell Activation 153
Naomi E. Harwood and Facundo D. Batista

Tracking the Dynamics of *Salmonella* Specific T Cell Responses..... 179
James J. Moon and Stephen J. McSorley

Imaging *Listeria monocytogenes* Infection *In Vivo* 199
Vjollca Konjufca and Mark J. Miller

Inflammation on the Mind: Visualizing Immunity in the Central Nervous System 227
Silvia S. Kang and Dorian B. McGavern

Multiphoton Imaging of Cytotoxic T Lymphocyte-Mediated Antitumor Immune Responses 265
Alexandre Boissonnas, Alix Scholer-Dahirel, Luc Fetler, and Sebastian Amigorena

Index..... 289

Contributors

Sebastian Amigorena

Institut National de la Santé et de la Recherche Médicale U653, Immunité et Cancer, Pavillon Pasteur, Institut Curie, 26 rue d'Ulm, 75245 Paris Cedex 05, France

sebastian.amigorena@curie.fr

Jeanette Ampudia

Department of Immunology and Microbial Science, The Scripps Research Institute, 10550 North Torrey Pines Rd., La Jolla, CA 92037, USA

Facundo D. Batista

Lymphocyte Interaction Laboratory, Cancer Research UK, London Research Institute, Lincoln's Inn Fields Laboratories, 44 Lincoln's Inn Fields, London WC2A 3PX, UK

facundo.batista@cancer.org.uk

Alexandre Boissonnas

Institut National de la Santé et de la Recherche Médicale U653, Immunité et Cancer, Pavillon Pasteur, Institut Curie, 26 rue d'Ulm, 75245 Paris Cedex 05, France

Andrew Bullen

Department of Pathology and Biological Imaging Development Center, University of California, 513 Parnassus Avenue, San Francisco, CA 94143-0511, USA

Andrew.Bullen@ucsf.edu

Jean-Pierre Clamme

Department of Immunology and Microbial Science, The Scripps Research Institute, 10550 North Torrey Pines Rd., La Jolla, CA 92037, USA

Michael L Dustin

Department of Pathology, Program of Molecular Pathogenesis, Skirball Institute of BioMolecular Medicine, NYU School of Medicine, 540 First Avenue, 2nd Floor, New York 10016, USA

Luc Fetler

Centre National de la Recherche Scientifique UMR 168, Laboratoire de Physico-Chimie Curie, Institut Curie, 26 rue d'Ulm, 75245 Paris Cedex 05 France

Reinhold Förster

Institute of Immunology, Hannover Medical School, Carl-Neuberg-Strasse 1, 30625 Hannover, Germany

Rachel S. Friedman

Department of Pathology and Biological Imaging Development Center, University of California, 513 Parnassus Ave, San Francisco, CA 94143-0511, USA

Guo Fu

Department of Immunology and Microbial Science, The Scripps Research Institute, 10550 North Torrey Pines Rd., La Jolla, CA 92037, USA

Nicholas R.J. Gascoigne

Department of Immunology and Microbial Science, The Scripps Research Institute, 10550 North Torrey Pines Rd., La Jolla, CA 92037, USA
Gascoigne@scripps.edu

Naomi E. Harwood

Lymphocyte Interaction Laboratory, Cancer Research UK, London Research Institute, Lincoln's Inn Fields Laboratories, 44 Lincoln's Inn Fields, London WC2A 3PX, UK

Il-Young Hwang

B-cell Molecular Immunology Section, Laboratory of Immunoregulation, NIAID, NIH, 10 Center Dr. Bethesda, MD 20892-1892, USA
jkehrl@niaid.nih.gov

Silvia S. Kang

National Institutes of Neurological Disorders and Stroke, National Institutes of Health, 10 Center Drive, Bldg 10, Rm 7C213, Bethesda, MD 20892, USA

John H. Kehrl

B-cell Molecular Immunology Section, Laboratory of Immunoregulation, NIAID, NIH, 10 Center Dr. Bethesda, MD 20892-1892, USA
jkehrl@niaid.nih.gov

Vjollca Konjufca

Washington University School of Medicine, Department of Pathology and Immunology, 660 South Euclid Avenue, St. Louis, MO 63110-1093 USA

Matthew F. Krummel

Department of Pathology and Biological Imaging Development Center, University of California, 513 Parnassus Avenue, San Francisco, CA 94143-0511, USA

Klaus Ley

La Jolla Institute for Allergy and Immunology, La Jolla, CA, USA

Carina Lotz

Department of Hematology, University Medical Center Utrecht,
Lundlaan 6, 3584EA Utrecht, The Netherlands

Michel Mallaun

Department of Biomedicine, University Hospital, Basel, Switzerland

Dorian B. McGavern

National Institutes of Neurological Disorders and Stroke, National Institutes of
Health (NIH), 10 Center Drive, Bldg 10, Rm 7C213, Bethesda, MD 20892, USA
mcgavernd@mail.nih.gov

Stephen J. McSorley

Medicine, University of Minnesota Medical School, Minneapolis, MN 55455,
USA

and

Center for Immunology, University of Minnesota Medical School, Minneapolis,
MN 55455, USA

and

Center for Infectious Diseases and Microbiology Translational Research,
University of Minnesota Medical School, Minneapolis, MN 55455, USA
mcsor002@umn.edu

Mark J. Miller

Washington University School of Medicine, Department of Pathology and
Immunology, 660 South Euclid Avenue, St. Louis, MO 63110-1093, USA
miller@pathology.wustl.edu

James J. Moon

Center for Immunology, University of Minnesota Medical School, Minneapolis,
MN 55455, USA

and

Department of Microbiology, University of Minnesota Medical School,
Minneapolis, MN 55455, USA

Nathalie Niederberger

Serono Pharmaceutical Research Institute, Geneva, Switzerland

Ed Palmer

Department of Biomedicine, University Hospital Basel, Switzerland

Chung Park

B-cell Molecular Immunology Section, Laboratory of Immunoregulation, NIAID,
NIH, 10 Center Dr. Bethesda, MD 20892-1892, USA

jkehrl@niaid.nih.gov

Vasily Rybakin

Department of Immunology and Microbial Science, The Scripps Research
Institute, 10550 North Torrey Pines Rd., La Jolla, CA 92037, USA

Alix Scholer-Dahirel

Institut National de la Santé et de la Recherche Médicale U653, Immunité
et Cancer, Pavillon Pasteur, Institut Curie, 26 rue d'Ulm, 75245 Paris Cedex 05,
France

Tim Worbs

Institute of Immunology, Hannover Medical School, Carl-Neuberg-Strasse 1,
30625 Hannover, Germany
worbs.tim@mh-hannover.de

Pia P. Yachi

Applied Molecular Evolution, 3520 Dunhill Street, San Diego, CA 92121, USA

Tomasz Zal

Department of Immunology, University of Texas, MD Anderson Cancer Center,
7455 Fannin, Houston, TX 77030, USA

Alexander Zarbock

Department of Anesthesiology and Intensive Care Medicine,
University of Münster, Münster, Germany
zarbock@uni-muenster.de

Two-Photon Imaging of the Immune System: A Custom Technology Platform for High-Speed, Multicolor Tissue Imaging of Immune Responses

Andrew Bullen, Rachel S. Friedman, and Matthew F. Krummel

Contents

1	Introduction.....	2
1.1	The Power of Imaging for Addressing Issues/Answering Questions in the Immune System.....	2
1.2	Functional Requirements for Imaging Immune Function <i>In Vivo</i>	5
1.3	Advantages of Multiphoton Imaging.....	9
2	Description of Custom Two-Photon Instrumentation.....	11
2.1	A Custom Design Composed of Off-the-Shelf Parts Simplifies System Construction.....	12
2.2	Optimizing Two-Photon Instrumentation.....	16
3	Representative Data.....	21
4	Future Perspectives.....	23
4.1	Pulse Manipulations.....	23
4.2	Alternative Scanning Methods.....	25
	References.....	26

Abstract Modern imaging approaches are proving important for addressing contemporary issues in the immune system. These approaches are particularly useful for characterizing the complex orchestration of immune responses *in vivo*. Multicolor, two-photon imaging has been proven to be especially enabling for such studies because of its superior tissue penetration, reduced image degradation by light scattering leading to better resolution and its high image quality deep inside tissues. Here, we examine the functional requirements of two-photon imaging instruments necessary for such immune studies. These requirements include frame rate, spatial resolution and the number of emission channels. We use this discussion as a starting point to compare commercial systems and to introduce a custom technology platform that meets these requirements. This platform is noteworthy because it is very cost-effective, flexible and experimentally useful. Representative data collected

A. Bullen (✉), R.S. Friedman, and M.F. Krummel
Department of Pathology and Biological Imaging Development Center, University of California
San Francisco, 513 Parnassus Ave, San Francisco, CA 94143-0511, USA
e-mail: Andrew.Bullen@ucsf.edu or Matthew.Krummel@ucsf.edu

with this instrument is used to demonstrate the utility of this platform. Finally, as the field is rapidly evolving, consideration is given to some of the cutting-edge developments in multiphoton microscopy that will likely improve signal strength, depth penetration and/or the experimental usefulness of this approach.

1 Introduction

Direct imaging of the individual cell types of the immune system in their native context undeniably provides the most accurate spatiotemporal assessment of the system-wide properties of the immune response. Over the past 6 years, this technique has increasingly been facilitated by imaging methods utilizing two-photon laser-scanning microscopy (TPLSM) (Cahalan and Parker 2008). Unlike other methods, the behavior of individual cells are observed via this technology in an largely intact microenvironment containing, by definition, physiological concentrations of soluble mediators, growth factors, as well as cell–cell contacts with other components of the system.

Central to this is the ability of multiphoton excitation to provide improved depth penetration and reduced phototoxicity over longer observation periods (Cahalan et al. 2002; Williams et al. 2001), which is a key aspect to observing biology over time within healthy tissues. To achieve such observational accuracy, however, is not without challenges. These include proper experimental design to highlight specific cells without perturbing the overall biology, optimal sample preparation to minimize artifacts due to whole animal surgery and, of course, the best possible instrumentation for detecting optical signals from the deepest possible location within complex organs. This latter component is an area of intense development and an area whose improvement simplifies experimental and sample-preparation considerations. In this review, we will highlight the optical and instrumentation approaches that are improving this technology, and compare a variety of TPLSM implementations used in immune-imaging. As an example of a custom system that has been highly successful in imaging immune responses, we will elaborate the details of a custom-instrument that we have implemented, and which is increasingly being adopted for its relative ease of implementation, flexibility, cost, and importantly, imaging quality. Finally, we will describe emerging technologies and how they are likely to improve spatial and temporal aspects of this approach.

1.1 The Power of Imaging for Addressing Issues/Answering Questions in the Immune System

What are the benefits of live-cell imaging in the immune response, generally? Studies undertaken by Wülfing and Davis (Wülfing et al. 1997), Delon and Trautmann (Delon et al. 1998), Negulescu and Cahalan (Negulescu et al. 1996)

and Dustin and Unanue (Dustin et al. 1997) in the mid-1990s highlighted the distinct power of observing single cell dynamics with reference to the calcium response. Notably, all these groups were able to take advantage of the fact that imaging single-cell dynamics permits the direct observation of an activation ‘timeline’. In particular, they were to observe each cell from the start of its interaction with an antigen-presenting cell, followed by the full course of activation and calcium influx dynamics as it related to cell shape change and motility arrest (Negulescu et al. 1996; Dustin et al. 1997; Delon et al. 1998), and subsequently how it was influenced by the nature of antigen-presenting cells (APC) (Delon et al. 1998) and peptide–MHC complexes (pMHC) (Wülfing et al. 1997).

The imaging of single events in their entirety provides clear benefits over other ‘bulk’ methods such as flow cytometry for observing kinetic relationships since it avoids the ‘temporal smear’ generated by variations in the population behavior. Take, for example, the onset, magnitude, and duration of calcium signaling in a population of cells. A variation within the population in any of these parameters can be both observed and normalized when all cells are measured in their entirety during the period of interest. In contrast, a bulk measurement of the population over time simply measures the average behavior. If there is great variation in any of the kinetic parameters, the maximum magnitude of the others can be misrepresented due to contributions from cells that are at different stages of the response. Analysis of single cells allows all parameters to be viewed in their direct relationship to each other (i.e., in the recording of each single cell). These can later be pooled by common feature for statistical analysis (e.g., always starting at the time of onset of the responses), thus providing dramatically improved details of downstream kinetic relationships within the population.

The direct observation of cells undergoing biological activity using real-time microscopy also provides important spatial information. This information can help describe subcellular events and/or characterize the local microenvironment. In the first case, direct imaging of immune cells *in vitro* permits subcellular analysis of responses, such as the very early imaging of antibody-driven calcium influx within cytotoxic T lymphocytes (CTLs). Such observations have provided evidence that much of the influx was polarized, emanating from a single side of the cell (Poenie et al. 1987). This is now known to represent release of intracellular calcium stores, often from polarized endoplasmic reticulum (ER). Similarly, the movement of subcellular signaling molecules within cells, tagged with GFP, permits the assembly of a wide variety of signaling complexes to be analyzed with reference to calcium signaling, morphology, and/or motility (Krummel et al. 2000; Schaefer et al. 1999; Bunnell et al. 2001; Varma et al. 2006; Yokosuka et al. 2005). In the second case, cellular behavior in complex tissues is not constant but rather varies depending on local factors such as the presence of chemokines. For example, naive T cells arrest more on dendritic cells (DC) that are already involved in activation via other T cells (Hugues et al. 2007; Castellino et al. 2006). This type of problem, in particular, has benefited from multiphoton imaging of immune responses *in vivo*.

Within this area, multiphoton microscopy has, or is poised, to address the following types of questions with respect to cellular activation:

- What are the single-cell dynamics of activation? For example, Miller and Cahalan (Miller et al. 2002, 2004), and Mempel and von Andrian (Mempel et al. 2004) have shown that T cells undergo activation in multiple phases, corresponding to initial scanning of antigen-bearing surfaces and culminating in firm arrest of T cells on activated DCs.
- Where does activation occur spatially within a given tissue? For example, it was found that B cells can be activated on DCs, following entry into the lymph node, and as they traverse the T cell zone rather than solely in B cell zone (Qi et al. 2006).
- What is the effect of the spatial milieu (different microenvironments or different tissues)? For example, activating B cells near the B cell zone/T cell zone junction are sensitive to a chemokine gradient in that zone which attracts them toward the T cell zone. In contrast, more distal cells show no evidence of motion toward this potential source of T cell ‘help’ (Okada et al. 2005).
- Which cell types are present during an immune response *in vivo* and how do they contribute? For example, DCs have been highlighted to be the partners for T cell activation using chemical dye-labeling *in vivo* (Miller et al. 2004), dye-labeling prior to their adoption (Mempel et al. 2004; Bousso and Robey 2003), antibody-labeling *in vivo* (Hugues et al. 2004), and genetic marking (Lindquist et al. 2004; Shakhar et al. 2005).

Multiphoton microscopy has the potential to produce multiple types of readouts. Currently, a majority is limited to determinations of cell–cell interactions and positional detail although improving instrumentation is now permitting greater use of subcellular markers. Such resolution and sensitivity will begin to allow direct measurements of signaling protein aggregation, endocytosis, exocytosis, and polarity, in addition to the creation of custom biosensors to report on specific signaling cascades. Some of the most frequently applied include:

- Cell arrest. For example, the arrest of T cells following exposure to antigen (Miller et al. 2002; Bousso and Robey 2003).
- Cell morphology. For example, T cells undergoing motility tend to do so in a hand-mirror morphology, similar to amoeba (Miller et al. 2002).
- Calcium influx. For example, B cells encountering antigen-bearing DCs upon entry into the lymph node can be observed to flux calcium as measured by Fluo4 (Qi et al. 2006). This method is limited at present as the fluorescent dyes for these types of studies are rapidly vesicularized.
- Cell–cell association (or persistence). For example, T cells activating in a lymph node often do so in ‘clusters’ (Bousso and Robey 2003; Tang et al. 2006; Beuneu et al. 2006; Sabatos et al. 2008) and such clusters can permit long-lived cell–cell contacts between adjacent cells leading to directed cytokine secretion (Sabatos et al. 2008).
- Subcellular analysis of particle distribution. For example, antigens taken up by macrophages in the cortical sinus are distributed within subcellular compartments there (Phan et al. 2007).

1.2 *Functional Requirements for Imaging Immune Function In Vivo*

Leukocytes have defined characteristics that define the requirements for imaging events *in vivo*. On the one hand, the immune system is highly motile and thus requires sufficiently fast sampling to quantify this motion. In addition, this is a system containing multiple cell types and, thus, requires multiple labeling and detection strategies to differentiate cell types. It is also not limited in its activity to the surface of tissues or organs – in fact the cells of the immune system can lie deep within tissues, surveying for or defending against foreign organisms.

Functional requirements that need be considered for imaging are speed of sampling, sensitivity of detection, particularly with reference to depth penetration, multicolor acquisition, and the tradeoff between all of these and microscopic spatial resolution and macroscopic field of view (FOV).

1.2.1 *Frame-Rate and Speed of Acquisition Considerations*

Lymphocytes, key players in the immune responses, are intrinsically motile, with center-of-mass displacements that reach $>25 \mu\text{m min}^{-1}$ (Miller et al. 2002). In addition, projections from the lymphocyte surface can appear and significantly change within seconds. As the path taken by T cells is rarely linear in tissues such as lymph nodes but more closely resembles a ‘random walk’ (Miller et al. 2002) (though it is not likely to be truly ‘random’; Bajenoff et al. 2006), higher sampling frequencies are essential to provide an accurate readout of instantaneous velocities. Regardless of the underlying guiding force for movement, it is clear that sampling frequency plays a large part in determining the accuracy of a measurement of velocity, particularly when cells are persistent for only a finite period of time. A brief practical measure is that the sampling interval t should be considerably less than the persistence time P .

As an illustrative example, consider theoretical displacements based on motion described by a typical equation for a Persistent Random Walk (Othmer et al. 1988):

$$\langle d(t)^2 \rangle = nS^2 [Pt - P^2 (1 - e^{-t/P})],$$

where $d(t)$ is the observed displacement, n is the number of dimensions, S is the speed, and P is the persistence (period of time without a turn). When the observed time period is less than the cellular directional persistence time ($t < P$), the equation reduces to:

$$d(t) = St$$

which is to say that the observed displacement is closely approximated by measures of speed multiplied by time. This is the ideal measurement scenario – that the measured displacement is in fact an accurate measure of the true instantaneous velocities.

For a theoretical cell with persistence of 2 min whose behavior followed this type of description (S set to 10), measurements at 30-s intervals ($P > t$) would yield displacement values of $5.8 \mu\text{m}/30 \text{ s}$ and therefore velocities of $11.6 \mu\text{m min}^{-1}$. Intervals of collection of 2 min ($P = t$) would on average obtain measurements of “instantaneous velocities” as $\sim 21 \mu\text{m} \text{ min}^{-1}$ or $10.5 \mu\text{m min}^{-1}$. Further reduced sampling rates of 4 and 10 min intervals ($P < t$) would on average obtain measurements of “instantaneous velocities” as 8.7 and $6.9 \mu\text{m min}^{-1}$, respectively. The true magnitude of the errors obviously depends upon the underlying biology and doubtless adheres to a significantly more complex description. Indeed, there are a plethora of variations of models for modeling cell motility (Codling et al. 2008). However, this example serves to indicate the value of fast sampling in theory, but may also indicate a practical explanation for modest differences in reported motility parameters for naive T lymphocytes depending upon the frame-rate of data acquisition.

In practice, lymphocytes can cover considerable distances during a short time course of analysis. This in turn creates the important consideration of total X–Y–Z FOV since one cannot track a cell that has left the observation volume. Practically, this will create conflicts with requirements for spatial resolution, since complete sampling of a larger volume can either be done by capturing more pixels (longer collection times) or with the same number of larger pixels. Practically, this often entails variations in the number of Z-slices that are collected since varying this parameter can quickly multiply the time taken to acquire data. For example, presuming 30 z-stacks are required to capture a sufficient volume of data for analysis, 3-s acquisition times result in a full 90 s-between frames, thus potentially under-representing the very fastest movements as described above. Lowering spatial resolution in the Z-axis by taking larger Z-steps may initially appear an attractive way to minimize these bottlenecks. However, the resulting decrease in ability to accurately assess the cell center of mass in the Z-axis results in inaccurate high and low velocities being reported and, more generally, a broadening of the velocity distribution. A more detailed analysis of the effect of both temporal and spatial sampling frequency on the accuracy of velocity measurements is presented in Codling and Hill (2005).

1.2.2 Number of Detection Channels

As the examples above illustrate, measurements of cells and their behaviors *in vivo* most frequently rely upon the relationships amongst cell types and their environment. Consequently, the number of detection channels should match the number of fluorescent tags. To this extent, a two-cell interaction requires at least two distinct channels in which to collect the fluorescence emissions from two distinct dyes. For example, interactions between T cells and DCs can be achieved using a red fluorophore (e.g., the vital dye CMTMR) to label T cells and the distinct green fluorophore (e.g., CFSE) labeling method for the DCs (Miller et al. 2004).

However, as the compartmentalization of the immune response is studied further, it becomes apparent that even a ‘simple’ organ like a lymph node comprises distinct zones and behaviors which vary according to those zones. This requires the use of additional fluorophores or combinations of fluorophores to highlight critical regions;

we term this fiduciary labeling as the fluorophore which thus serves to highlight key positions within organs and tissues. So, for example, activating B cells near the T–B border move toward the border as a result of gradients of CCR7 ligands whereas those that are a distance away fail to do so – despite both being within the same B cell follicle (Okada et al. 2005). Additional fluorophores that highlight this border (in this case those that highlight the T cell zone) prove useful in determining the spatially distinct behavior. As another example, T cells in ectopic EL-4 tumors tend to migrate along paths parallel to blood vessels. Markers that highlight the blood vessels are necessary to reveal this – otherwise the T cells show guided migration without any mechanistic insight behind the nature of this confinement.

Thus, the use of fiduciary labeling leads to a frequent need to provide at least a third channel. More complex biology (i.e., those involving more than two cell types plus obligate fiduciary labels) can easily require 4 or more channels and this should be considered for choosing or adapting a microscope. In practice, the number of fluorophores and thus channels does not need to equal the number of distinct species to be labeled due to the possibility for multiplexing. In this way, three cell types can be labeled using combinations of just two dyes (green, red and green–red together create three distinct species in just two channels). As a general rule, the number of populations that can be distinctly labeled can be defined as:

$$C = 2^n - 1$$

where C is the number of distinct species that can be separately distinguished based on binary determinations of the presence of a dye and n is the number of channels of distinct detection. In practice, the true number that can be distinguished depends a bit on the application. For example, if labeled species (e.g., cells) never get very close, then different levels of each dye can be introduced into collections of cells leading to much larger variation in species and thus discrimination. As an example, Lichtman and colleagues generated populations of neurons *in vivo* using differing levels of CFP, YFP, and dsRed (three fluorophores) which permitted discrimination of approximately 90 different ‘colors’ based on combinations of just these three (Livet et al. 2007). On the other hand, the ability to discriminate based on quantitative measures of each component (component analysis) is made more difficult by fluorophores with wide-emissions that ‘bleed’ light into each other’s emission channels and thus somewhat resemble ‘dual-colored species’. Component analysis can often still distinguish these, except when cells or structures bearing fluorophores get very close to one another. When species overlap in the same measurement space (i.e., voxel), the quantitative contributions also blur and it is often difficult to tease apart the borders of the two. Under such circumstances, more distinct fluorophores may be required.

1.2.3 Detection Sensitivity

A critical requirement for effective deep-tissue imaging of immune cells is efficient detection of emission light. There are two aspects of detection sensitivity: detector sensitivity and detection path efficiency. In general, there are two main detector options:

photomultiplier tubes (PMTs) and charge-coupled device (CCD) cameras. CCD cameras typically have better quantum efficiency, the ability to convert light into electrical signals suitable to digitize. However, while both detector types can have high gain capabilities, PMTs often excel in multichannel and scanning applications because they combine good sensitivity with a large measurement bandwidth. PMT-based systems are also less affected by scattering in the emission path because fluorescence is assigned to a particular point in the sample based on its instantaneous excitation time rather than by its position at the detector. Additionally, PMT number scales more cheaply than increases in camera number. This is particularly important for systems employing three or four emission channels. While it is possible to combine a CCD camera with an emission filter wheel to get spectral separation this results in considerably higher total collection times since each volume of data needs to be illuminated multiple times. This in turn can affect the overall collection speed and increase the likelihood of photobleaching and phototoxicity at the sample.

The nature of the detection path also determines the collection efficiency of the optical system and is therefore an important parameter. The detection path extends from the back aperture of the objective lens through to the detector itself. From an optical design perspective, short detection paths generally provide the greatest collection efficiency. Furthermore, the correct choice of dichroic mirrors and barrier filters along this path are critical to maximizing total detection efficiency, minimizing the detection of autofluorescent wavelengths and minimizing bleed-over or crosstalk between emission channels.

1.2.4 Number of Lasers

Another way to distinguish between different fluorescent species (and thereby discriminate between more cell types or fiduciary species) is to employ different excitation wavelengths. Switching between different excitation wavelengths is not easily achieved with current Ti-sapphire lasers. However, we and a number of other groups have begun to integrate multiple lasers into a single system. While not a cheap option, this approach benefits from the ability to excite more fluorophores and distinguish between fluorophores with overlapping emission spectra but resolvable excitation spectra. However, simultaneously illuminating a sample with two lasers increases the likelihood of phototoxicity and complicates the discrimination of fluorophores with overlapping excitation spectra. For this reason, dual or multiple laser systems typically require recording from interlaced frames, which increases the amount of time required to scan the sample and thus decreases the overall collection rate.

1.2.5 Depth Penetration

Much of the interesting biology of the immune response occurs below the surface of organs. Unfortunately, most mammalian tissues scatter visible light significantly

and do so in a wavelength-dependent fashion. Measured scattering constants (μ_s) are typically of the order of 50 cm^{-1} (Collier et al. 2003). The probability of transmission T of the photon without redirection by scattering after a path length L (cm) is given by the equation:

$$T = e^{-\mu_s L}.$$

Under these circumstances, at depths of just $50 \mu\text{m}$, approximately 25% of the incident beam is typically scattered (and lost) during excitation and a similar percentage is redirected during fluorescence emission. This rises to 40% at $100 \mu\text{m}$ and 72% at $250 \mu\text{m}$ making such depths practically inaccessible.

Additionally, tissue is not just scattering but also absorptive of both incident light and emitted fluorescence, an effect that is linearly related to the tissue thickness (depth) subtended during excitation. Absorption is also highly dependent on the wavelength of incident light (or fluorescence) and is somewhat tissue specific. Typically, visible light is more likely to be absorbed. In fact, it has long been recognized that there exists an “optical window” (i.e., 600–700 nm) where major cell and tissue absorbers, such as melanin and hemoglobin, exhibit the least amount of absorbance (König 2000). This optical window has been exploited by many *in vivo* microscopic techniques (Frangioni 2003).

Scanning of the sample (vs full field illumination), coupled with collection at a PMT, permits spatial assignment of all of the measured emitted light intensity. This occurs regardless of the scattered path this light takes en route to the PMT and thus effectively eliminates a large portion of emission scatter. However, the most critical feature in deep tissue is absorption and this is where many confocal approaches often fail. In practice, imaged depths of up to $100 \mu\text{m}$ have been reported with spinning disk (Egeblad et al. 2008) or even scanning-based confocal microscopy (Stoll et al. 2002). The former, when operated up to these depths, can sometimes be significantly better than multiphoton imaging as a result of the larger quantum efficiencies of current-generation cascade-based CCD cameras (as compared to PMTs). There can also be some overall benefit in resolution at shallow depths due to the combined effects of lower wavelengths used in single-photon and confocal pinhole on the overall point-spread function. However, starting around $50 \mu\text{m}$ in many tissues, the scatter into adjacent pixels (blurring) combined with the loss of incident excitation light due to single-photon absorption becomes unacceptably high.

1.3 Advantages of Multiphoton Imaging

While many forms of optical imaging can be used to study the immune system, multiphoton imaging has many clear advantages. These advantages include superior tissue penetration, less image degradation by light scattering leading to better resolution, and high image quality deep inside tissues. Furthermore, tissue autofluorescence elicited with infra-red (IR) excitation is significantly reduced over equivalent visible

Table 1 Current multiphoton instrument options

Source	Scanning mechanism		Detector	Colors	Sensitivity	Imaging rate (fps)	Spatial resolution (max. lines per image)	Pulse conditioning	Ease of implementing	Cost
	X and Y	Z (range)								
Custom	Parker-Sanderson	Resonant + galvo	PMT	2 4	High	Up to 60	400	No Yes	Difficult Moderate	\$\$\$
	Krummel-Bullen	Dual galvo	PMT	2	High	2	???	No	Difficult	\$\$\$
	Svoboda	Dual galvo	PMT	2	High	3	512	No	Difficult	\$\$\$
Mixed ¹	Kleinfield	Focus drive automation	PMT	1 + 1 ³	High	2	512	No	Moderate	\$\$\$\$
	Yuste ²	Dual galvo	PMT	3	High	2	512	No	Moderate	\$\$\$\$
Commercial	Ridsdale ⁴	Dual galvo	PMT	2 or 3	High	5	Up to 6,144 per dimension	Nonstandard	Easy	\$\$\$\$\$
	Zeiss LSM 710 NLO	Dual galvo	PMT	2	High	4	64–4,096 per dimension	Yes	Easy	\$\$\$\$\$
	Olympus FV1000 MPE	Dual galvo	PMT	4	High	1 ⁵ or 25 ⁷	8,196 ⁸ or 512 ⁹	Nonstandard	Easy	\$\$\$\$\$
	Lecia TCS SP5 MP	Tandem systems ⁵	PMT	2 or 3	High	1 ¹¹ or 30 ¹²	512	Nonstandard	Easy	\$\$\$\$
	Prairie Ultima	Tandem systems ¹⁰	PMT	1 ¹⁴	Low	\$30 ¹⁵	1,000 ¹⁶	Yes	Easy	\$\$\$\$\$
LaVision TriM Scope	Multibeam	Piezo ¹³	CCD camera							

¹Adaptation of existing commercial system

²Modification of Olympus Fluoview microscope

³One detector for fluorescence and one for SHG signal

⁴Modification of Nikon C1 confocal scope

⁵Tandem scanning system includes dual galvos scanner and resonant scanner operating in bidirectional scan mode

⁶Using dual galvo scanner

⁷Using fast resonant scanner

⁸Using dual galvo scanner

⁹Using fast resonant scanner

¹⁰Tandem scanning system includes dual galvos scanner and acoustic optic scanner.

¹¹Using dual galvo scanner

¹²Using acousto optic scanner

¹³Signal limited to first 150 μm

¹⁴More possible with extra camera and/or emission filter wheel

^{15,16}Depends on CCD camera

wavelengths, which improves signal specificity and image brightness against background. When compared to confocal systems, multiphoton systems typically exhibit better optical efficiency with no signal loss arising from an emission pinhole. So, while absolute signal magnitude is typically less when compared to confocal applications, the overall signal-to-noise ratio is typically improved. Multiphoton excitation also produces highly resolved z excitation planes that leads to extremely good z-registration and consequently better three dimensional reconstructions. This localized excitation also produces lower levels of photodamage (i.e., toxicity) and thereby allows increased recording episodes. In short, the tissue penetrating power of infrared light makes multiphoton excitation especially suitable for *ex vivo* and *in situ* imaging.

Multiphoton imaging systems are available in many forms. These options include commercial systems, user adaptations of existing confocal microscopes, and custom systems. Many of these current options and the relative merits of each type are documented in Table 1. Current commercial two-photon imaging systems are commonly extensions of existing confocal microscopes and therefore enjoy the advantages of being commercial grade instruments with the flexibility to perform different kinds of imaging.

In contrast, custom-built systems can be constructed at a considerably reduced cost and offer greater potential for customization. In particular, they offer the ability to quickly add extra features and improved capabilities. There are also several free software packages [e.g., ScanImage (Pologruto et al. 2003) and MPscope (Nguyen et al. 2006)] available that facilitate the construction of these custom-built systems. Existing confocal microscopes can also be retrofitted by users to become two-photon scopes, and there are several reports documenting how this can be done (e.g., Fan et al 1999; Majewska et al. 2000; Nikolenko et al. 2003; Ridsdale et al. 2004).

2 Description of Custom Two-Photon Instrumentation

We have assembled a scanning two-photon system based on a resonant scanner as first used by Tsien and colleagues (Fan et al. 1999). Our design was modeled after second generation resonant scanner designs by Ian Parker and Mike Sanderson (Sanderson and Parker 2003; Callamaras and Parker 1999). Their early designs functioned as confocal systems but more recent incarnations extend the technology (and actually simplify the design) for two-photon excitation (Nguyen et al. 2001). In addition to minor modifications in the overall design of the Parker/Sanderson prototypes, our instruments have been expanded to include four PMTs and also place those PMTs within the infinity space of the objective. Four-channel collection (and higher channel numbers) are now possible using high-speed acquisition cards. Furthermore, as we are essentially biologists first, our system is facilitated by a collection of scan-head parts available from Sutter Instruments. This availability dramatically reduces the need for novices to construct parts.

2.1 *A Custom Design Composed of Off-the-Shelf Parts Simplifies System Construction*

The important elements in this design are shown schematically in Fig. 1. Generally, this system can be assembled from readily available parts. Each of these parts and their important properties are discussed below. Additional and more detailed information regarding this design is available on our website (<http://pathology.ucsf.edu/krummel/2PhotonHome.html>). Included on this site is a comprehensive parts list.

2.1.1 Laser

Highly specialized lasers are required for multiphoton excitation. In particular, this type of excitation requires the concentration of photons in space and time. Spatial concentration of photons is normally achieved by focusing a laser beam to a small spot with a high numerical aperture objective lens as in traditional single-photon microscopy. In contrast, the temporal concentration of photons is accomplished by compressing photons from a continuous source into ultra-short (i.e., femtosecond) pulses. Near-infrared pulses of this type are commonly produced by a Ti-sapphire oscillator driven by a continuous-wave pump laser and typically exhibit high peak intensities but low average power.

Early Ti-sapphire lasers were notable for their limited wavelength range and poor user friendliness. In particular, these early systems were intolerant to variations

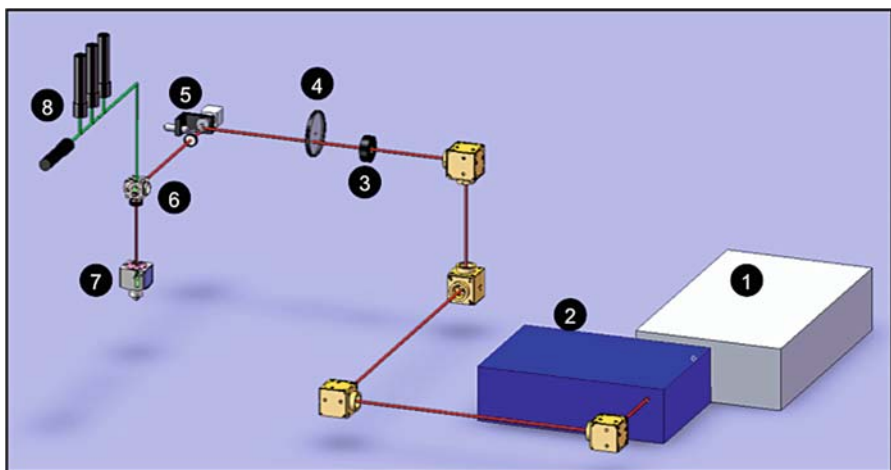


Fig. 1 Instrument design scheme including: (1) Ti-sapphire laser; (2) pulse conditioner; (3) mechanical shutter; (4) neutral density filter wheel; (5) scanning mirrors; (6) primary dichroic mirror; (7) z-focus drive including objective; and (8) PMTs

in room temperature and required constant adjustment. Now, however, there are modern one-box solutions that encompass both the pump laser and the regenerative amplifier which perform more robustly. These systems have simplified laser control and operation to the point where everyday laser operation no longer requires a specialized laser technician.

Likewise, extended range Ti:Sapphire lasers are now available that give access, and sufficient power, to a wider spectral range (700–1,040 nm). This is important for those interested imaging with red fluorescent protein (RFP) and other indicators that require longer excitation wavelengths. This improved spectral bandwidth also enables the use of more fluorophores within the same experiments.

Our multiphoton imaging systems all employ some version of the Newport/Spectraphysics Maitai product, but equivalent lasers from other suppliers are available that perform similarly. This laser has a pulse length of approximately of ~100 fs and is clocked at 80 MHz. Lasers are available that possess shorter pulse lengths and in theory these may improve multiphoton excitation provided that these pulses can be propagated all the way to the sample. These Ti-sapphire systems also come in a range of sizes. Typically, 6-W systems produce sufficient power to support most kinds of imaging. Because of the nature of this laser, and the downstream imaging hardware, it is firmly mounted to a large vibration isolation table.

2.1.2 Pulse Conditioning Unit

Immediately downstream of the laser is a pulse-conditioning unit that prechirps the femtosecond pulses in a way that maximizes the efficiency of multiphoton excitation. The role of this device and its utility is described in a later section. We have employed two different version of this technology: firstly, a freestanding device from APE (Berlin, Germany) called FemtoControl, and secondly, on a separate system, we have installed an add-on called DeepSee, from Newport/Spectraphysics, to an existing Ti-sapphire laser. Both systems are functionally equivalent.

2.1.3 Translation Optics

The beam steering optics used in this design translate the laser beam between devices laid out on a large vibration isolation table. Typically we have chosen to use optical components that are optimized for ultra-fast laser applications (mostly from Newport Corporation). These broadband optics are designed to operate over the spectral range, and at the power levels, of the Ti-sapphire laser while exhibiting maximizing reflectivity and minimizing pulse dispersion.

2.1.4 Scanning Mirrors

The vast majority of laser scanning microscopes use galvanometer mirrors. They have excellent optical properties and allow zooming and image rotation. Their major

drawback is their relatively slow speed (>1 ms per line). Resonant mirrors are an alternative often used for high frame rate imaging. We have chosen to use a dual configuration including a fast (8 kHz) resonant scanner for fast line scans (CRS) and a slower closed-loop galvanometric scanner for vertical scanning (M3S). Bi-directional horizontal scanning enables line scans of approximately ~ 60 μs in duration which corresponds to video rate imaging with 480 lines per image. We obtained both these scanning mirrors from General Scanning Inc. (GSI; Billerica, MA). Each scanner is under the control of custom electronics also supplied by GSI. These electronics, power supplies and related hardware required to synchronize this system with the video acquisition board are contained within a mirror control box (Sutter Instruments, Novato, CA). These scanners are mounted on an optical breadboard enclosed within a scanning enclosure. This enclosure was also manufactured by Sutter Instruments and is mounted adjacent to Olympus BX51 microscope base.

One problem with these resonant mirrors is that they introduce some image distortion that requires digital correction. This distortion arises because the mirror velocity is not linear but rather has a sinusoidal profile. The pixel manipulation and field selection required to overcome this image distortion is conducted automatically behind the scenes and is transparent to the user. Details of the mathematical procedure underlying this correction have been described extensively elsewhere (Sanderson 2004; Leybaert et al. 2005).

2.1.5 Objectives, Field Size and Stage Movement

The objective lens(es) used with this system determines the level of spatial resolution and the efficiency of signal capture. Any lens considered must also be able to work in media or physiological fluids and possess sufficient working distance for use with tissues and animals. Moreover, it must exhibit high transmittance for both the pulsed IR excitation light and a wide range of emitted fluorescence. We predominantly use an XLUMP FL20XW from Olympus. This objective combines intermediate magnification (20 \times) with relatively high NA (0.95) and is particularly well suited for imaging in scattering tissue.

This system also possesses electronic control of the field size. The user is able to choose between two pixel sizes (i.e., 0.4 or 0.7 $\mu\text{m pixel}^{-1}$). Correspondingly, the field size scanned is either 192×160 μm or 336×280 μm .

While most of the experimental work conducted on this system is focused on a microscopic level of detail, there are instances where users want to combine both microscopic and macroscopic levels of resolution. This is achieved by stage scanning with a motorized stage (Prior 101A, Boston, MA). This process is automated and controlled in software (described below).

2.1.6 PMT Selection

Photomultiplier tubes are hand-made devices with a surprising amount of batch-to-batch variability in their signal- and noise-amplification characteristics. While each supplier typically provides average values for sensitivity and noise performance,

these can be misleading. In particular, root-mean-square (rms) measurements of noise performance are essentially time-averages that disguise significant peak-to-peak signal fluctuations. In high bandwidth applications, such as video rate scanning, short but significant bursts of noise, which are undetectable in rms measurements, become significant problems. For example, in a system collecting pixels at MHz frequency, we have observed PMTs with transient bursts of noise lasting just a microsecond or two that cause isolated pixels to become completely saturated. Depending on the frequency of these bursts, such PMTs may prove unsuitable for imaging. Some suppliers allow batches of 10–20 PMTs to be individually tested as part of a purchase. In general, there continues to be advances in the development of lower-noise, high gain PMTs. For instance, some latest generation GaAs-based detectors have shown exceptional sensitivity and signal-to-noise performance. However, such PMTs can also become easily saturated and transiently insensitive. This places an additional burden on the user to carefully manage their light levels to avoid such damage.

2.1.7 Emission Split Allows Four-Color Imaging

The four emission channels included in this design provide coverage of most of the visual spectrum normally used for fluorescence imaging. A scheme showing the specifics of these individual channels is documented in Fig. 2. The spectral placement of these channels allows one to collect signal from four independent fluorophores. Moreover, the relative placement of these filters was chosen to (1) match the spectra from currently available fluorescent proteins, (2) provide the best spectral separation between fluorophores, and (3) to maximize the signal capture in each channel. With our current hardware, there is some flexibility to switch emission filters and thereby fine-tune these channels even further, but changing dichroic mirrors is more difficult. In cases where the spectra of two fluorophores overlap in adjacent channels, it is possible, via image math, to separate out the underlying contribution of each indicator. Likewise, linear unmixing can be used to remove the contribution of autofluorescence or overlapping signals. Examples of these procedures are shown in below Fig. 6.

2.1.8 Software

Our system employs several different software applications from multiple vendors. These applications are run on two separate computers and in turn connect to several devices or control boxes. A scheme documenting the relationships between these computers, applications and devices is shown in Fig. 3. Coordination of these disparate elements during image acquisition is achieved by a single master application (Confocal; IO Industries, London, Ontario, Canada). The Confocal application controls the scheduling and relative timing of all the hardware devices used in a typical experiment. It also interacts with a commercial video recording software suite (i.e., VideoSavant) that is used to reconstruct and record images.

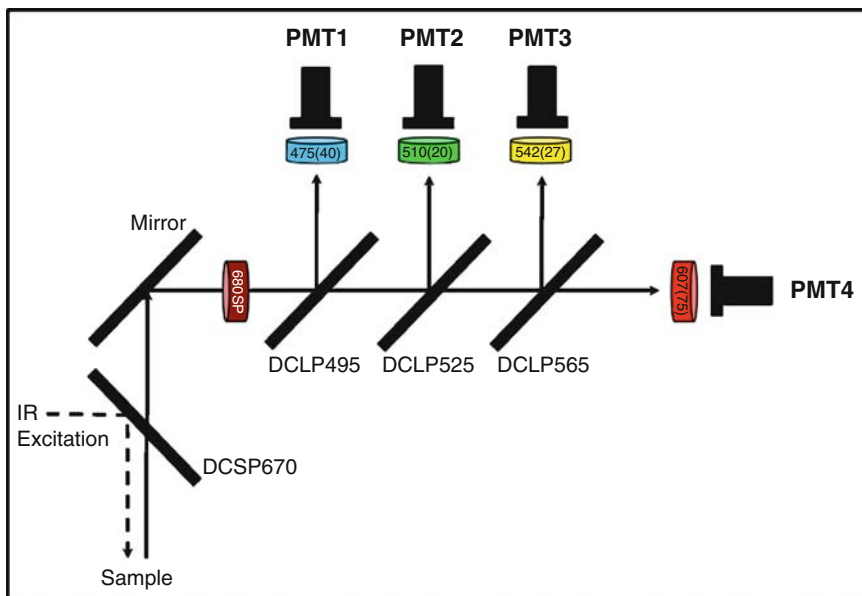


Fig. 2 Emission split. This optical configuration is optimized to capture the maximum fluorescence signal from commonly used fluorescence proteins (especially CFP, GFP, YFP and dsRed or similar). This setup includes a strong excitation blocking filter that excludes any backscattered excitation light without impacting the emitted fluorescence. *DCSP* Dichroic short-pass mirror, *DCLP* dichroic long-pass mirror. Barrier filters described by their center wavelength (and full width at half maximum)

The graphical user interfaces of these programs are shown in Fig. 4. The confocal application is composed of a Main tab and three derivative tabs. Data can be acquired as a single time point, a z-series, a z-series over time, or any of the above using multiple stage positions. Files are exported in multiimage TIFF format that is accessible to Image J, Metamorph, Imaris, and the simpler Windows image viewers.

2.2 Optimizing Two-Photon Instrumentation

It is relatively common nowadays to be able to buy, or retrofit, an existing confocal microscope with a laser suitable for multiphoton excitation. However, such instruments provide relatively poor imaging capabilities and many are unable to achieve the necessary frames rates described earlier. Furthermore, the relative efficiency of IR delivery and fluorescence capture in these systems is often suboptimal. Based on these factors and others we have learned from experience, the following section describes several critical considerations in achieving high quality multiphoton images and physiologically relevant results.

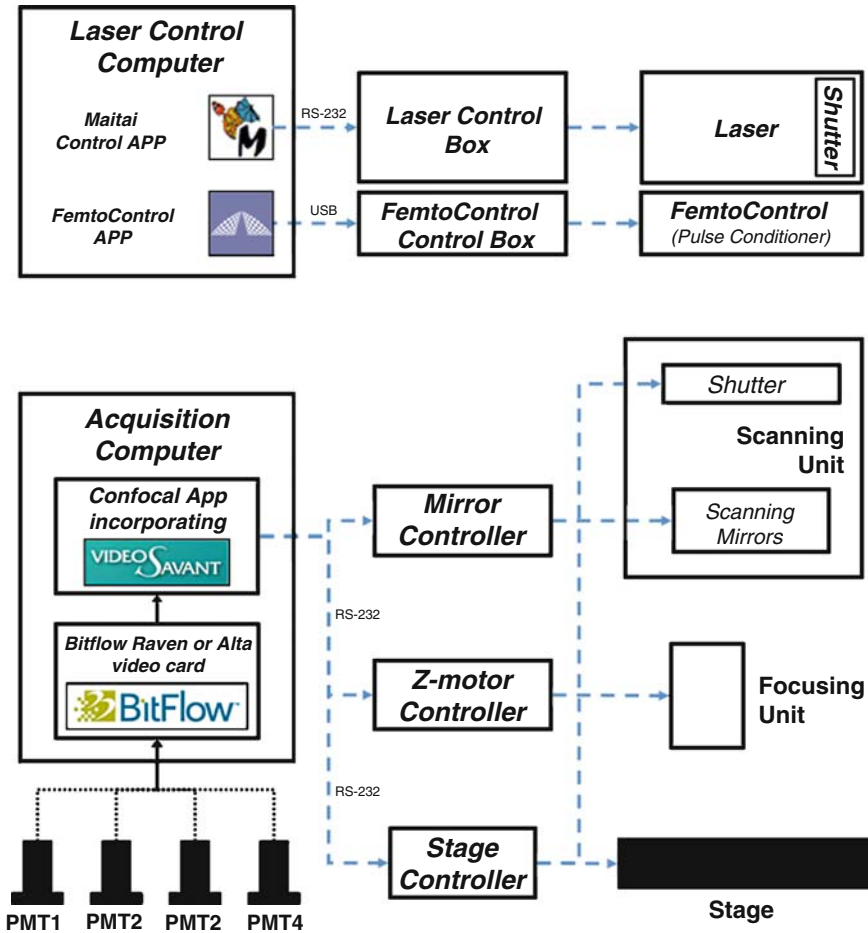


Fig. 3 Software control scheme showing the relationship between the acquisition and laser control computers, device control boxes and each physical device in the larger system. Dotted blue lines represent outbound control signals. Black lines represent acquired or processed signals

2.2.1 A Simplified Light Path Minimizes the Effect of Dispersion

The strength of multiphoton excitation is inversely proportional to pulse duration. Although very short pulses (<100 fs) give the strongest signal, they are no longer purely monochromatic and, as they propagate through different optical elements (i.e., optical fibers and objective lens), some dispersion, or pulse broadening, occurs. This chromatic dispersion arises because separate spectral components are retarded differentially depending on their wavelength. Pulse dispersion reduces the overall efficiency of multiphoton excitation in general but is most

a



b

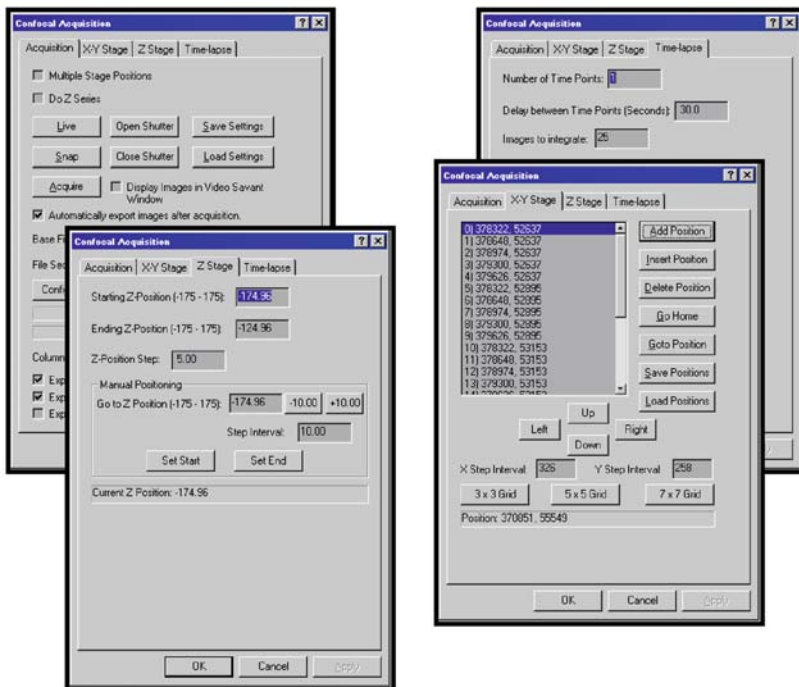


Fig. 4 Software user interface. (a) Applications running on the laser control computer. (b) Different control tabs of the Confocal application running on the acquisition computer

problematic in applications that use complicated optical configurations such as intravital microscopy (IVM). In theory, pulses of greater starting intensity could be used to overcome dispersion, but these can cause photodamage. Similarly, pulse power can be amplified at the expense of repetition rate (Theer et al. 2003) but again, only under conditions in which photodamage or background fluorescence are not limiting.